Hindawi
International Journal of Antennas and Propagation
Volume 2019, Article ID 9705406, 9 pages
https://doi.org/10.1155/2019/9705406

Research Article

Rapid Simulation of Temporal-Spatial Correlated 3D Sea Clutter

Ye Zhao,[1,2] **Peng-Ju Yang**,[1,2] **Xin-Cheng Ren**,[1,2] **and Xiao-Min Zhu**[1,2]

[1]*School of Physics and Electronic Information, Yan'an University, Yan'an 716000, China*
[2]*Shaanxi Key Laboratory of Intelligent Processing of Big Energy Data, Yan'an 716000, China*

Correspondence should be addressed to Ye Zhao; zhaoye07074135@163.com

Received 9 October 2019; Accepted 2 December 2019; Published 24 December 2019

Academic Editor: Raffaele Solimene

Due to the difficulties in actual measurement of sea clutter and uncertainties of experimental data, the electromagnetic (EM) scattering model becomes a better alternative means to acquire the sea clutter. However, the EM scattering model still faces the problems of huge memory consumption and low-computational efficiency when dealing with the large size of sea surface or the long time case. Thus, this paper presents a statistical model to simulate the temporal-spatial correlated three-dimensional (3D) sea clutter, which is based on the statistical properties obtained from the EM scattering model, such as probability density function and correlation function. The comparisons show that the texture feature, autocorrelation function, and PDF of the sea clutter simulated by the statistical model have a good agreement with the results given by the EM model. Furthermore, the statistical model is with high efficiency and can be used to simulate the large scene or long time temporal-spatial correlated 3D sea clutter.

1. Introduction

It is the basic working mechanism of radar to discover and identify the target by using the electromagnetic (EM) scattering characteristics of the target. While the target exists or is hidden in the surrounding environment, the interference caused by the EM scattering of environment to the detection of the radar target signal is called radar clutter. Certainly, the radar echo from the sea surface environment is sea clutter. Because the sea surface is affected by the wind force, environmental humidity, surge, and other natural factors, the sea clutter signal has complex changes and high intensity. In addition, the sea surface is dynamic and constantly changing and the wave movement of sea surface has a rather complex relationship with the environmental factors, such as wave valley, ripple, vortex, and spray, all of which will affect the scattering characteristics of sea surface. Usually, in order to eliminate or reduce the influence of sea clutter, it is necessary to simulate sea clutter to obtain the distribution characteristics of sea clutter under various conditions before the radar detects the target on the sea surface. Moreover, the study on the characteristics of sea clutter is also of great significance for the natural mechanism explanation of the sea clutter and radar system design.

At present, sea clutter modelling, suppression, and target detection under the background of sea clutter are one of the hotpots in the research of EM scattering of the sea surface [1, 2]. For the sea clutter modelling, a reasonable and practical sea clutter simulation model is very important, which can offset the difficulties in actual measurement of sea clutter and uncertainties of experimental data. Accordingly, many sea clutter simulation models based on the EM scattering model have been developed, such as Kirchhoff Approximation (KA) [3, 4], two-scale model (TSM) [5, 6], small slope approximation (SSA) [7–9], and some other facet-based models [10, 11]. Among these approaches, KA is just valid for the lower incident angle. TSM, as a famous and frequently-used tool, could only give an average of the scattering coefficient. The SSA method confronts the difficulties of huge memory consumption and low-computational efficiency, due to that the required sampling interval of sea surface in SSA is too small, such as less than one-eighth of the incident EM wavelength. Comparatively speaking, the facet-based asymptotical model (FBAM) [11] is a superior method and could give the scattering field information of single facet on sea surface which includes both amplitude and phase. In the FBAM, the sea surface is envisaged as a two-scale profile, in which the large-scale gravity wave is approximately

decomposed by a mount of slightly rough facets with capillary waves as their microscopic random roughness. Because of considering the scattering of capillary waves, the computing time will increase when calculating the EM scattering from a sea surface with large area. In short, the EM scattering models mentioned above are harder to deal with the scattering of sea surface with large area or long time case.

Another kind of sea clutter simulation models are based on the statistical model, such as the zero-memory nonlinear transform (ZMNL) [12, 13] and spherically invariant random process (SIRP) [14, 15]. And it is the core step of the sea clutter simulation based on the statistical model to generate the correlated non-Gaussian random process with the specified statistic and correlation properties [16–18], such as probability density function (PDF), correlation function, or spectral density function. In this paper, the FBAM is adopted as the EM scattering model to generate the sea clutter and then acquire the statistic and correlation properties for the establishment of a statistical model in the subsequent. However, in traditional sea clutter simulations, the sea clutter is always simulated as the time sequence or the two-dimensional (2D) sea clutter [17, 18] (in time-range dimensions or range-azimuth dimensions). With the development of the techniques of high-resolution imaging and target detection, the traditional time sequence or 2D sea clutter simulations cannot satisfy the practice requirement. Thus, the simulation of the temporal-spatial correlated three-dimensional (3D) (in range-azimuth-time dimensions) sea clutter will have a very important academic and realistic significance.

The rest of this paper is organized as follows. Section 2 gives two kinds of simulation models, namely, the EM scattering model and statistical model, to generate temporal-spatial correlated 3D sea clutter. And the statistical model is detailedly described here, which extends the ZMNL method to the 3D case. Section 3 gives some numerical results including the generation of 2D spatial correlated and 3D temporal-spatial correlated sea clutter. And then, the comparisons of the texture feature, statistical characteristics, and consumed time between the EM scattering model and the statistical model are shown. Section 4 forms the conclusion.

2. Simulation Models for 3D Sea Clutter

2.1. EM Scattering Model. For the simulation of 3D sea clutter, the FBAM proposed in our earlier work [11] is an available EM scattering model, which has been very well validated. It not only can be used to the RCS prediction and Doppler spectrum analysis of the sea surface [19], but also can be applied to the composite scattering and synthetic aperture radar (SAR) imagery simulation from a ship target over a sea surface [20].

In FBAM, the sea surface is composed by a mount of tilted slightly rough facets. The scattering field from an arbitrary rough facet takes the following expression:

$$\mathbf{E}(x,y,t) = \frac{k^2(1-\varepsilon)}{2iR} e^{ikR} \cdot \widetilde{\mathbb{F}}_{PQ} \cdot \mathbf{I}(\cdot), \tag{1}$$

where k is the wave number of electromagnetic waves; R is the position vector of facet; $\widetilde{\mathbb{F}}_{PQ}$ is the polarization factors related to the relative dielectric constant ε of sea water and Fresnel reflection coefficients ($P, Q = H, V$ denote the polarization of incident and scattering waves, respectively); and $\mathbf{I}(\cdot)$ is an integral of the surface profile within a facet. The detailed expressions of $\widetilde{\mathbb{F}}_{PQ}$ and $\mathbf{I}(\cdot)$ can be found in [11], which are omitted here due to space limitations.

2.2. Statistical Model. In this part, the ZMNL method is extended to the 3D case for establishing a statistical model, which contains two major operational procedures, that is, the simulation of the correlated Gaussian process of zero mean and unit variance, and the generation of the desired non-Gaussian process using the nonlinear transformation.

For the 3D case, the spectral density function $S(k_x, k_y, \omega)$ and autocorrelation function $R(\rho_x, \rho_y, \tau)$ of the stochastic field consist of a pair of Wiener–Khintchine relationships, similar to the 2D case [21], which is given by

$$\begin{aligned} R(\rho_x,\rho_y,\tau) = {} & \int_{-\infty}^{\infty}\int_{-\infty}^{\infty}\int_{-\infty}^{\infty} S(k_x,k_y,\omega) \\ & \cdot e^{-i\left(k_x\rho_x + k_y\rho_y + \omega\tau\right)} \mathrm{d}k_x \mathrm{d}k_y \mathrm{d}\omega, \end{aligned} \tag{2}$$

$$\begin{aligned} S(k_x,k_y,\omega) = {} & \frac{1}{(2\pi)^3} \int_{-\infty}^{\infty}\int_{-\infty}^{\infty}\int_{-\infty}^{\infty} R(\rho_x,\rho_y,\tau) \\ & \cdot e^{i\left(k_x\rho_x + k_y\rho_y + \omega\tau\right)} \mathrm{d}\rho_x \mathrm{d}\rho_y \mathrm{d}\tau, \end{aligned} \tag{3}$$

where k_x and k_y are wave numbers, ρ_x and ρ_y are separation distances in two directions. ω is angular frequency, and τ represents time interval. Then, the 3D correlated Gaussian process $g(x, y, t)$ can be expressed by the following series as $M, N, L \longrightarrow \infty$, namely,

$$g(x,y,t) = \sum_{m=-M}^{M}\sum_{n=-N}^{N}\sum_{l=-L}^{L} A_{mnl} \cdot \cos\left(k_{xm}x + k_{yn}y + \omega_l t + \phi_{mnl}\right), \tag{4}$$

where ϕ_{mnl} are independent random phase angles selected from a uniform distribution over $[0, 2\pi]$. A_{mnl} is proportional to the square root of the spectral density function at (k_m, k_n, ω_l):

$$\begin{aligned} A_{mnl} &= \left(2S(k_{xm},k_{yn},\omega_l)\cdot\Delta k_x\cdot\Delta k_y\cdot\Delta\omega\right)^{1/2}, \\ k_{xm} &= m\cdot\Delta k_x, \quad m = -M,\ldots,M, \\ k_{yn} &= n\cdot\Delta k_y, n = -N,\ldots,N, \\ \omega_l &= l\cdot\Delta\omega, \quad l = -L,\ldots,L, \end{aligned} \tag{5}$$

$$\begin{aligned} \Delta k_x &= \frac{k_{ux}}{M}, \\ \Delta k_y &= \frac{k_{uy}}{N}, \\ \Delta\omega &= \frac{\omega_u}{L}. \end{aligned} \tag{6}$$

In (6), k_{ux}, k_{uy}, and ω_u represent the upper cut-off wave numbers and frequency in corresponding dimensions of the $k_x - k_y - \omega$ coordinates, respectively.

If a stochastic field (e.g., $\mathbf{E}(x, y, t)$) is given, then the discretized version of spectral density function $S(k_x, k_y, \omega)$ of this field can readily be calculated by using the fast Fourier transform (FFT) algorithm. And the autocorrelation function of this stochastic field can be obtained easily based on (2) through the FFT algorithm. Namely, the correlation properties of an arbitrary stochastic field can be acquired by executing the FFT algorithm twice.

So, assuming that the desired correlation properties (i.e., the correlation properties of $\mathbf{E}(x, y, t)$) are available, the correlated 3D Gaussian process $g(x, y, t)$ of zero mean and unit variance can be generated according to (3) and (4). Then, the desired non-Gaussian process $f(x, y, t)$ can be generated by executing nonlinear transformation from the correlated 3D Gaussian process, which takes the following calculation:

$$f(x, y, t) = F_{\text{non-G}}^{-1}\{F_G[g(x, y, t)]\}, \tag{7}$$

where $F_G[\cdot]$ represents the cumulative distribution function of Gaussian process $g(x, y, t)$ and $F_G(x) = (1/2)[1 + \text{erf}(x/\sqrt{2})]$. $F_{\text{non-G}}^{-1}\{\cdot\}$ is the inverse cumulative distribution function of non-Gaussian process $f(x, y, t)$. If the non-Gaussian process $f(x, y, t)$ follows the log-normal distribution with the shape parameter σ and scale parameter μ, the inverse cumulative distribution function of $f(x, y, t)$ can be expressed as

$$F_{\text{non-G}}^{-1}\{x\} = \exp\left[\sqrt{2}\sigma \times \text{erf}^{-1}(2x - 1) + \mu\right]. \tag{8}$$

So, (7) can be rearranged to give the following expression:

$$f(x, y, t) = \exp[\sigma \times g(x, y, t) + \mu]. \tag{9}$$

In theory, the stochastic fields $\mathbf{E}(x, y, t)$ and $f(x, y, t)$ have consistent texture feature, correlation function, and PDF.

3. Results and Discussion

Figure 1 is given here to validate the performance of the FBAM in the simulation of the PDF of the time series of sea clutter and the prediction of backscattering coefficient. The incident frequency is 14 GHz at VV polarization, and the wind is upwind at speed of 5 m/s. For the generation of the time series of sea clutter, the incident angle is $\theta_i = 30^\circ$. Comparisons between the FBAM and experiment [22] indicate that the FBAM is a better EM model to generate the sea clutter and then acquire the statistical properties.

Next, we simulate the sea clutter to verify the performance and efficiency of the statistical model.

3.1. Two-Dimensional Case. In order to verify the statistical model, Figure 2 gives the comparisons of amplitude and autocorrelation function of 2D (in range-azimuth dimensions) spatial correlated sea clutter generated by statistical and EM models. For the EM model simulation, the incident frequency is 5 GHz slanting at the incident direction of $\theta_i = 40^\circ, \phi_i = 0^\circ$, and the results are completed in the backscattering case and for HH polarization. The 2D sea surface is generated based on the Monte Carlo method [23] using the Elfouhaily et al.'s spectrum [24], the sampling number along the x and y directions is $M = N = 128$, the size of the facet is $\Delta x = \Delta y = 0.8$ m, the wind is upwind at speed of 5 m/s, the time $t = 0$ s, the relative dielectric constant of the sea water is calculated by the Klein model [25] at 20°C, and 35‰ salinity. In addition, the simulated 2D spatial correlated sea clutter by the EM model is of log-normal distribution and with the shape and scale parameters of $3.565560E-01$ and -4.407049, respectively. For ease of comparison, the desired correlation properties in the statistical model simulation should be consistent with the simulated 2D spatial correlated sea clutter by the EM model.

From Figure 2, it could be obviously found that the amplitude and autocorrelation function of 2D spatial correlated sea clutter generated based on the statistical and EM models have a consistent texture feature. In order to give a more intuitive comparison, the comparisons of 1D plot of the autocorrelation function and PDF are shown in Figure 3. It is seen that 1D plot of the autocorrelation function and PDF of 2D spatial correlated sea clutter generated by the statistical model agree well with the results simulated by the EM model.

Compared with the EM model, the major advantage of the statistical model is that it could quite efficiently generate sea clutter in a very large size of scene. Figure 4 compares the amplitude and autocorrelation function of 2D spatial correlated sea clutter generated by the statistical model with different sizes of scenes. For clearer comparison, Figure 5 gives the comparisons of 1D plot of the autocorrelation function and PDF. From Figure 5, one can see that, the correlation in the edge of scene becomes smaller with the increase of scene and the middle area of the larger scene has a consistent correlation with the small scene. Besides, the sea clutter with different sizes of scenes has a consistent PDF (the amplitude and autocorrelation function of $100\text{ m} \times 100\text{ m}$ are shown in Figure 2(a)).

Furthermore, in order to contrast the efficiency between the statistical and EM models, Table 1 gives the time taken by the above two models in the simulations of 2D sea clutter with different sizes of scenes. Obviously, the statistical model is with high efficiency, which is because that the FFT technique is used in the statistical model to generate the correlated sea clutter.

3.2. Three-Dimensional Case. The simulation of 3D temporal-spatial correlated sea clutter is similar to the simulation of 2D spatial correlated sea clutter. For the EM model simulation in the 3D case, the parameters are same with the 2D case except that the sampling number at t direction is 128 and the time interval is 0.1 s. Besides, it should be explained that the simulated 3D temporal-spatial correlated sea clutter by the EM model is of log-normal distribution and with the shape and scale parameters of $3.563838E-01$ and -4.405951, respectively.

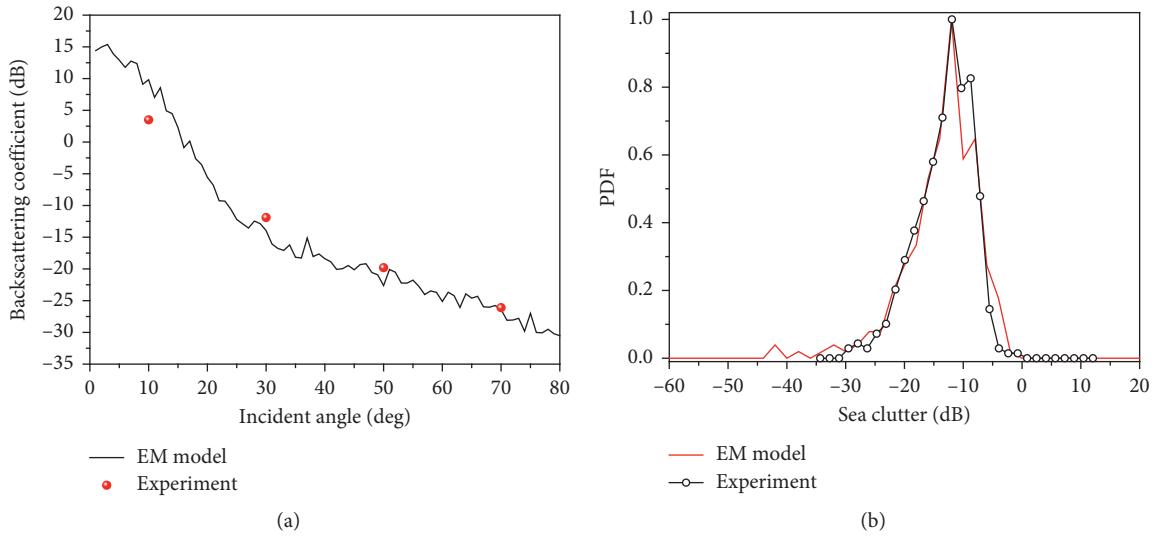

Figure 1: Validations on the performance of the FBAM. (a) Backscattering coefficient. (b) PDF of the time series of sea clutter.

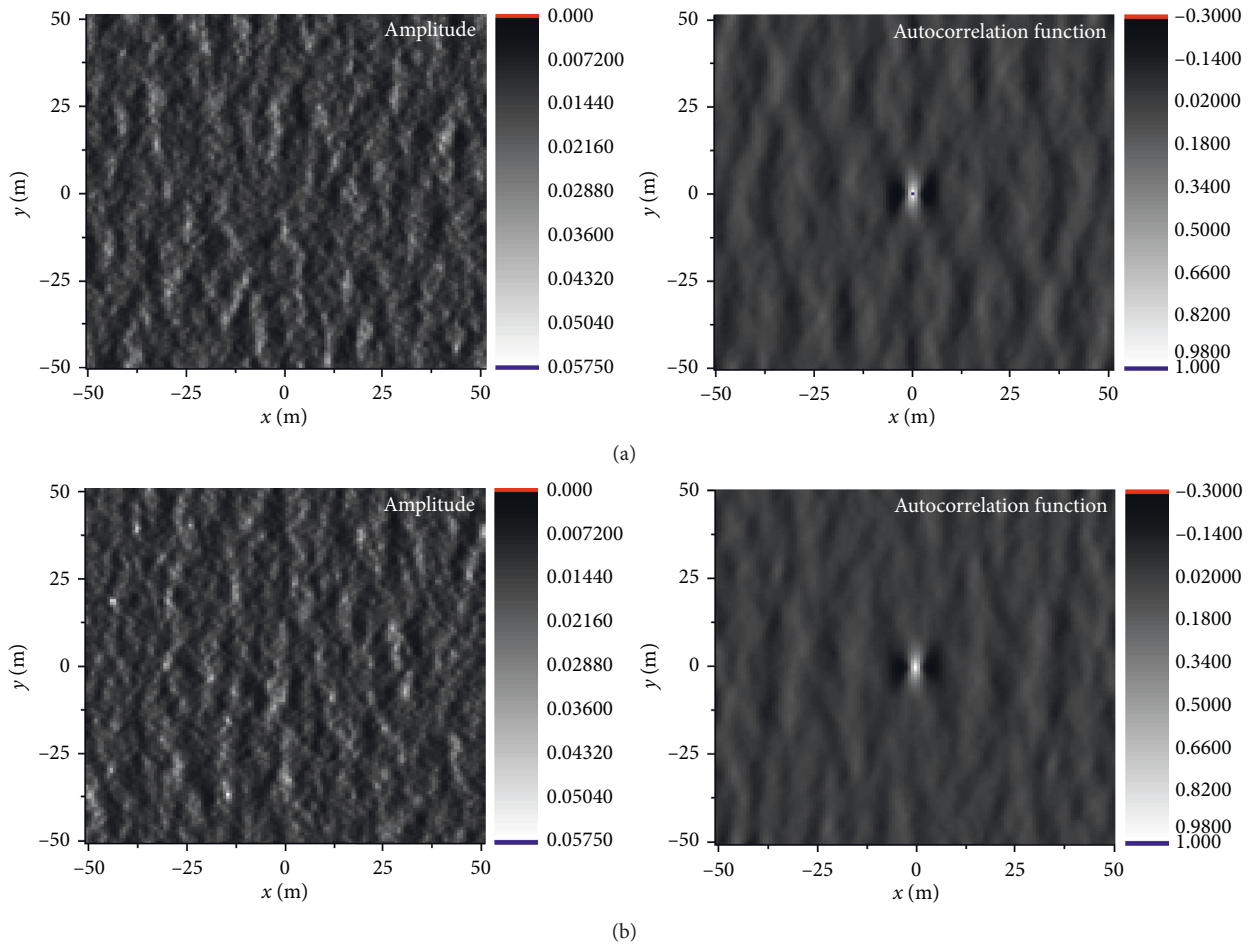

Figure 2: Comparisons of amplitude and autocorrelation function of 2D sea clutter generated by statistical and EM models. (a) Statistical model. (b) EM model.

Figure 6 gives the amplitude and autocorrelation function of 3D temporal-spatial correlated sea clutter generated by the statistical model in *xOt* plane, *xOy* plane, and *yOt* plane, respectively. It is seen from Figure 6 that the amplitude and autocorrelation function in different planes have different textures. Figure 7 shows the comparison of 1D

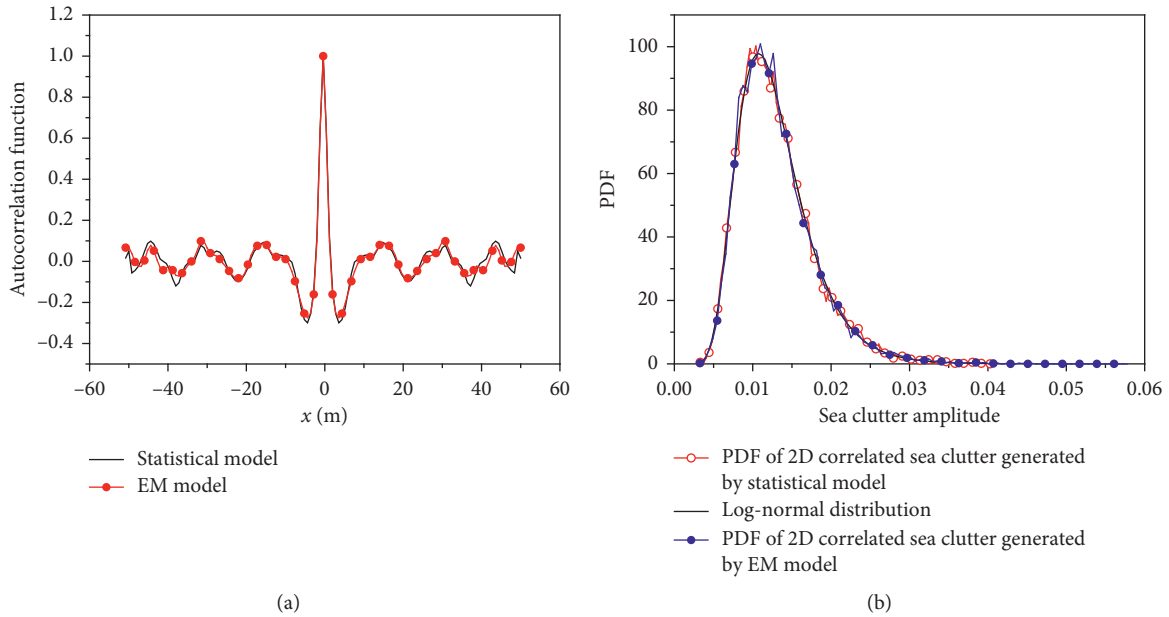

Figure 3: Comparisons of 1D plot of the autocorrelation function and PDF of 2D sea clutter generated by statistical and EM models. (a) 1D plot of the autocorrelation function. (b) PDF.

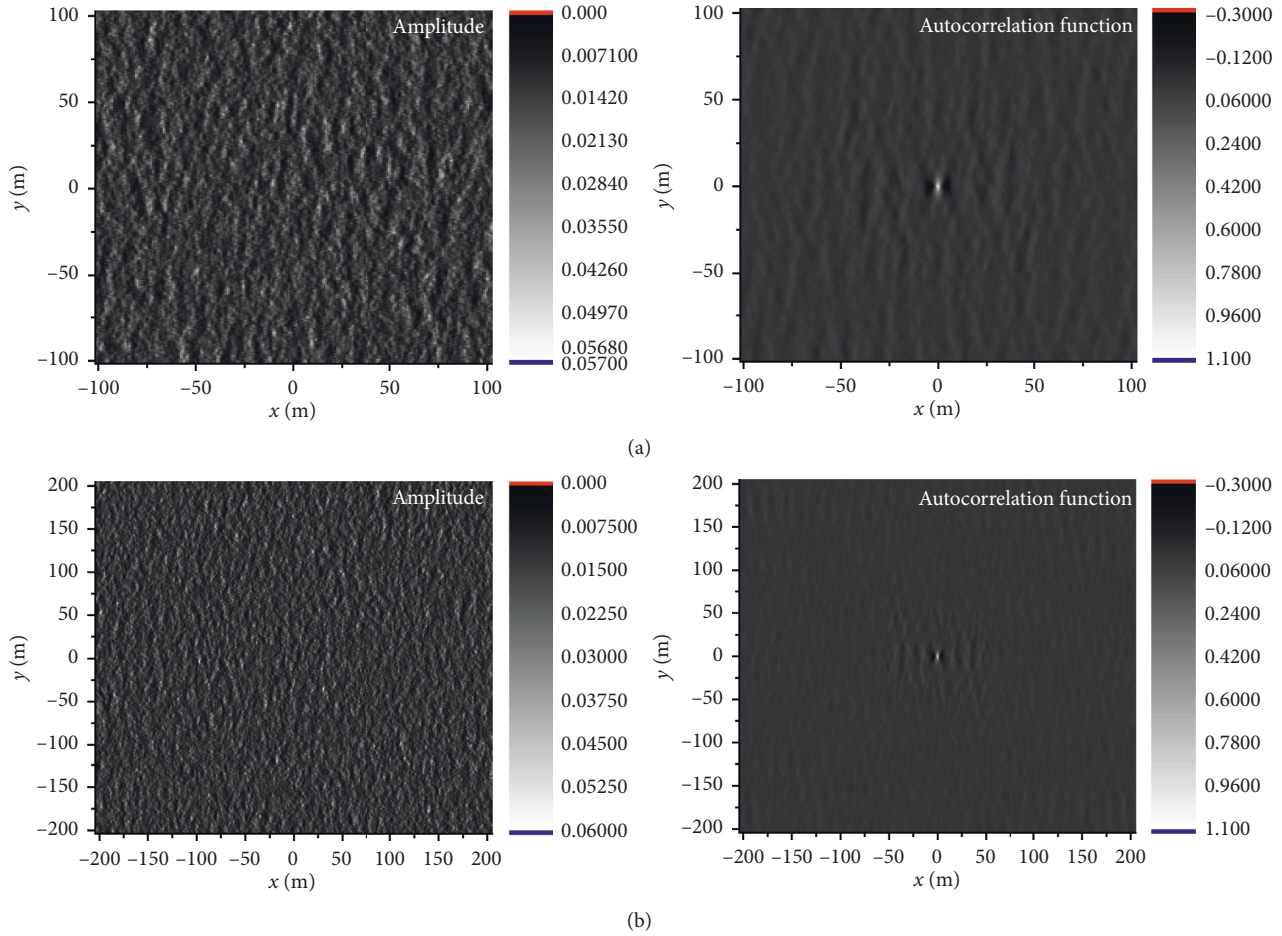

Figure 4: Comparisons of amplitude and autocorrelation function of 2D sea clutter by the statistical model with different sizes of scene. (a) 200 m × 200 m. (b) 400 m × 400 m.

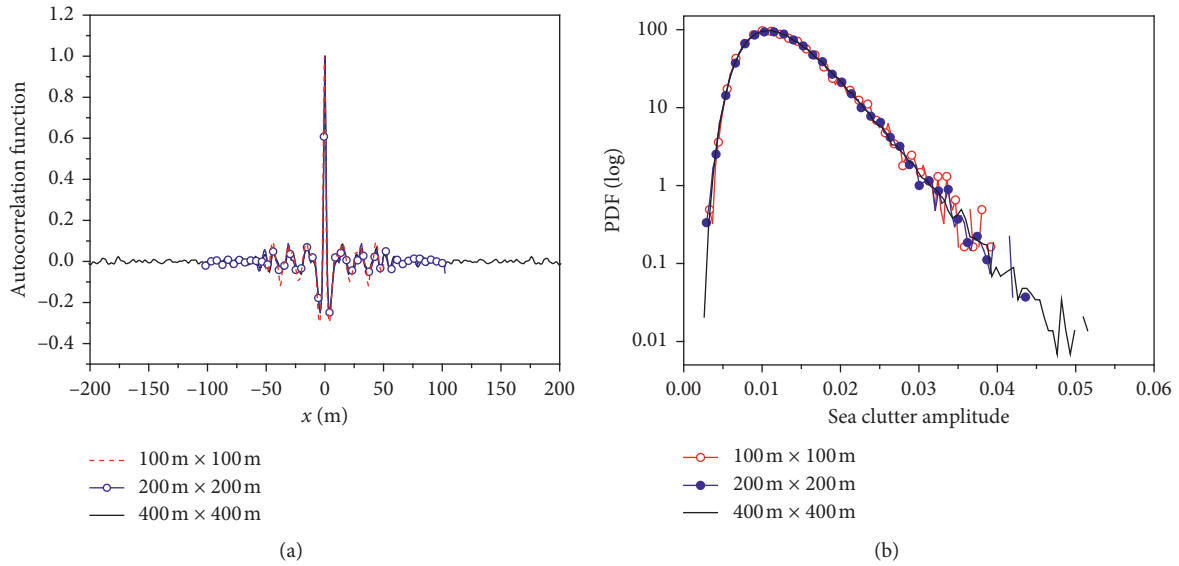

Figure 5: Comparisons of 1D plot of the autocorrelation function and PDF of 2D sea clutter by the statistical model with different sizes of scenes. (a) 1D plot of the autocorrelation function. (b) PDF.

Table 1: Comparison of the consumed time in the simulations of 2D sea clutter with different sizes of scenes.

The size of scene (m^2)		100×100	200×200	400×400
Time (sec)	Statistical model	0.025	0.0765	3.0779
	EM model	4.67	18.05	70.11

*Calculated by a computer with Intel(R) Core(TM) i7-6700 CPU @ 3.40 GHz.

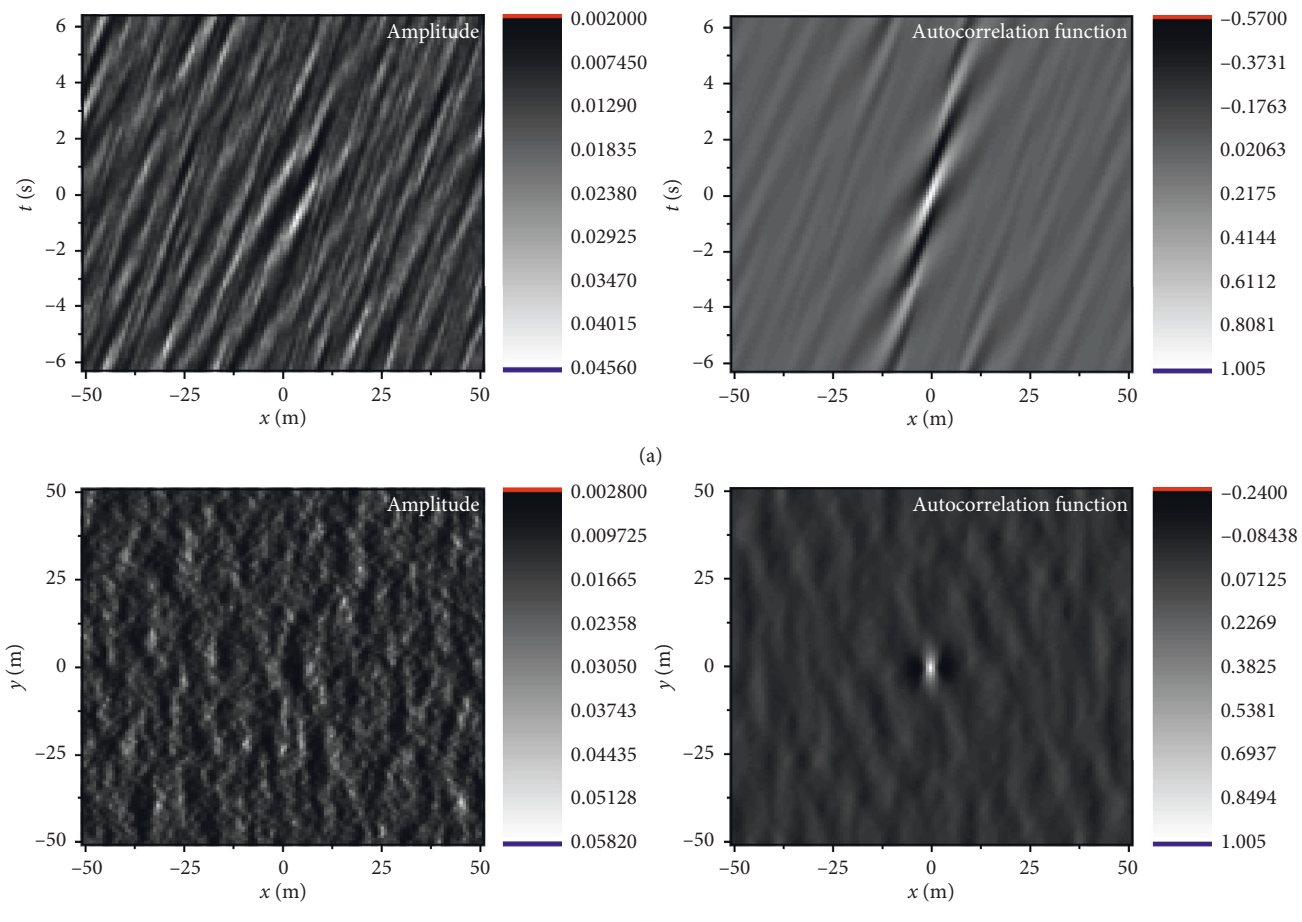

Figure 6: Continued.

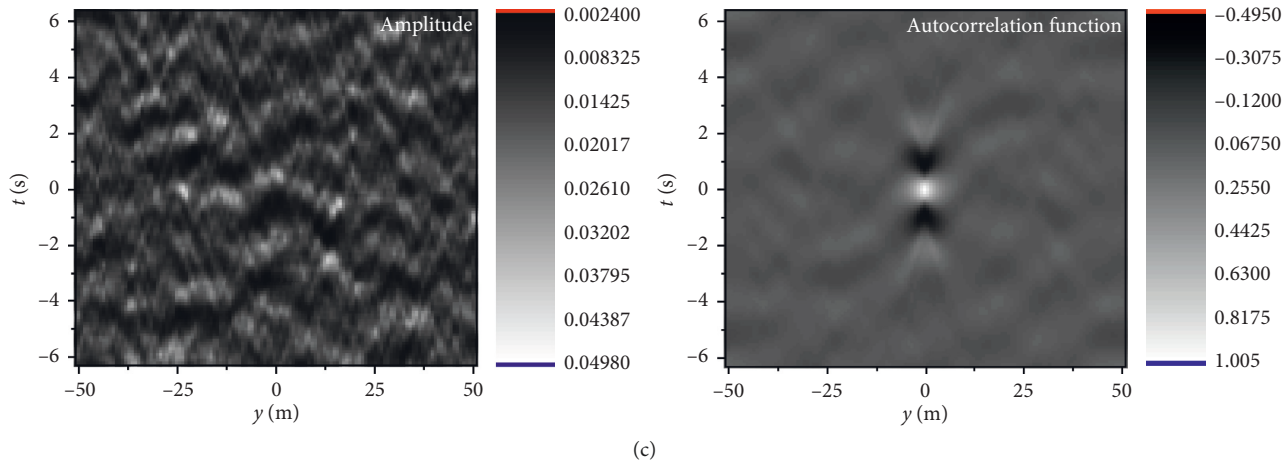

Figure 6: The amplitude and autocorrelation function of 3D sea clutter by the statistical model. (a) *xOt* plane. (b) *xOy* plane. (c) *yOt* plane.

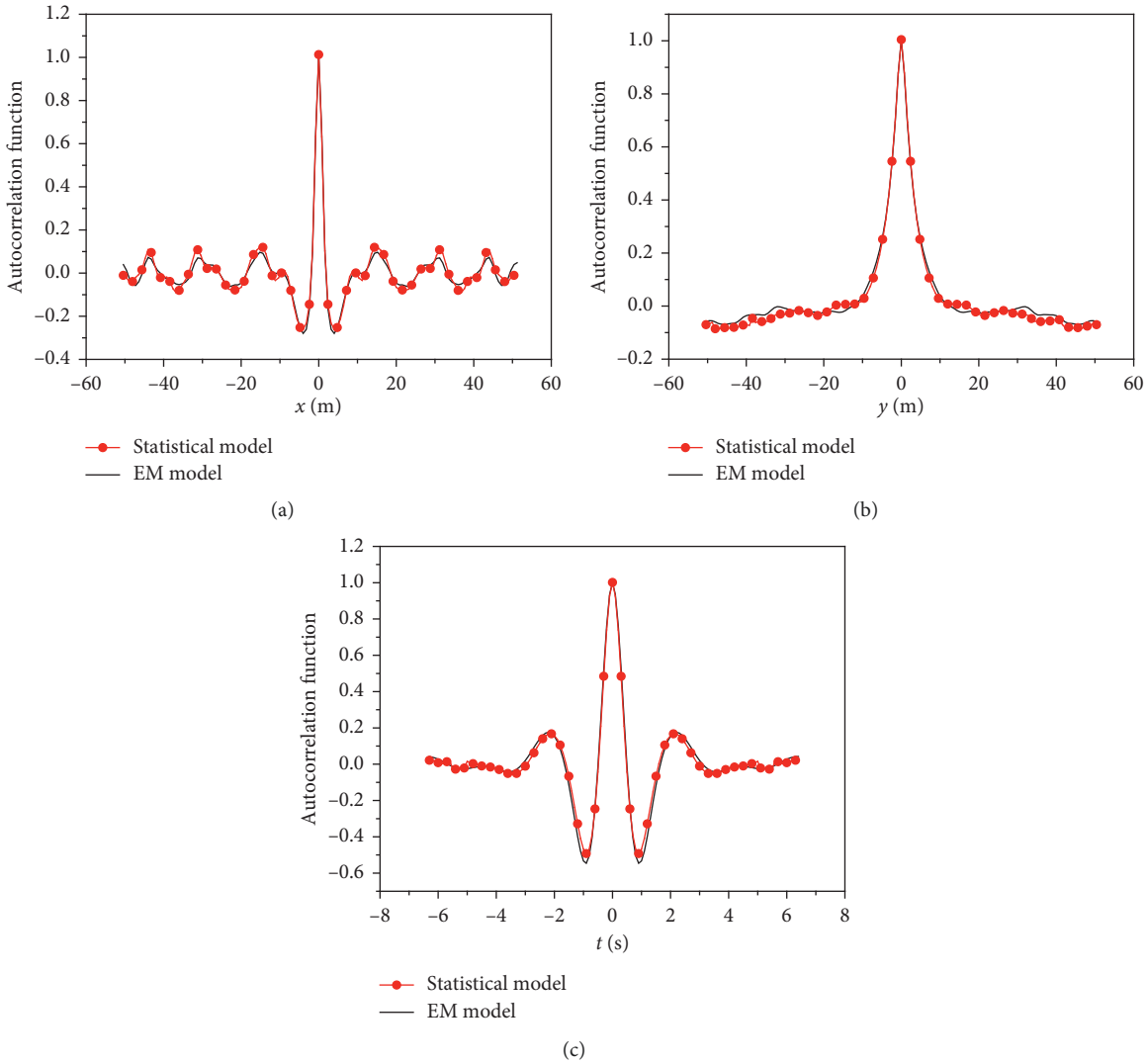

Figure 7: Comparison of 1D plots of the autocorrelation function of 3D sea clutter at *x*, *y*, and *t* direction between statistical and EM models.

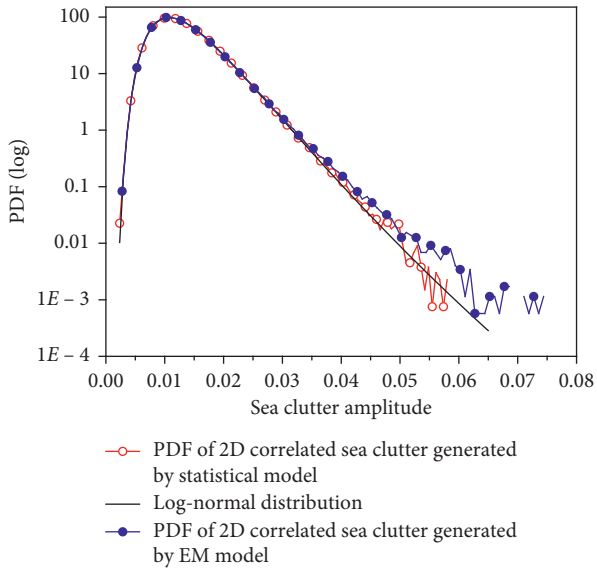

Figure 8: Comparisons of PDF of 3D sea clutter between statistical and EM models.

Table 2: Comparison of the consumed time in the simulations of 3D sea clutter with different sizes of scenes and sampling number at t direction.

The size of scene (m^2)		50×50			100×100	200×200
Sampling number at t direction		128	256	512	128	128
Time (sec)	Statistical model	1.81	3.56	7.79	7.37	28.92
	EM model	14.56	29.73	59.18	58.68	234.66

*Calculated by a computer with Intel(R) Core(TM) i7-6700 CPU @ 3.40 GHz.

plots (i.e., at x, y, and t direction, respectively) of the autocorrelation function of 3D temporal-spatial correlated sea clutter between statistical and EM models. Accordingly, the comparison of PDF is illustrated in Figure 8. From Figures 7 and 8, it is seen that 1D plots of the autocorrelation function and PDF of 3D temporal-spatial correlated sea clutter generated by the statistical model agree well with the results simulated by the EM model.

In order to contrast the efficiency of the statistical and EM models in the simulations of 3D sea clutter, Table 2 gives the comparison of the consumed time in the simulations of 3D sea clutter with different sizes of scenes and sampling number at t direction. As shown in Table 2, the statistical model increases efficiency about eight times.

The above simulation results of 2D and 3D cases could demonstrate that the statistical model is valid and can be used to quite efficiently generate the correlated sea clutter in a very large size of scene or the long time case.

4. Conclusions

In this paper, a statistical model extended from the ZMNL method to the 3D case is proposed to simulate the temporal-spatial correlated 3D sea clutter. And the statistical and correlation properties obtained from the EM scattering model are the foundations of the statistical model. The simulation results show that the texture feature, autocorrelation function, and PDF of the sea clutter simulated by the statistical model have a good agreement with the results given by the EM model. And the comparisons of the consumed time in the simulations of 2D and 3D sea clutter could demonstrate that the statistical model can quite efficiently simulate the large scene or long time temporal-spatial correlated 3D sea clutter. Besides, the proposed statistical model may facilitate the investigations on the natural mechanism explanation of sea surface scattering, sea clutter suppression, and target detection. These relevant studies will be under consideration in further research work.

Data Availability

The simulation data used to support the findings of this study are included within the article.

Conflicts of Interest

The authors declare that they have no conflicts of interest.

Acknowledgments

This work was supported in part by the National Natural Science Foundation of China (Grant nos. 61801416, 61861043, and 61701428), Natural Science Basic Research Plan in Shaanxi Province of China (Grant nos. 2019JQ-237 and 2019JQ-120), Shaanxi Provincial Education Department (Grant no. 18JK0872), Scientific Research Foundation of Yanan University (Grant no. YDBK2016-16), and Open Foundation of Fudan University Key Laboratory for Information Science of Electromagnetic Waves (MOE) (Grant no. EMW201910).

References

[1] H. W. Melief, H. Greidanus, P. van Genderen, and P. Hoogeboom, "Analysis of sea spikes in radar sea clutter data," *IEEE Transactions on Geoscience and Remote Sensing*, vol. 44, no. 4, pp. 985–993, 2006.

[2] F. Luo, D. Zhang, and B. Zhang, "The fractal properties of sea clutter and their applications in maritime target detection," *IEEE Geoscience and Remote Sensing Letters*, vol. 10, no. 6, pp. 1295–1299, 2013.

[3] E. I. Thorsos, "The validity of the Kirchhoff approximation for rough surface scattering using a Gaussian roughness spectrum," *The Journal of the Acoustical Society of America*, vol. 83, no. 1, pp. 78–92, 1988.

[4] A. Ishimaru and J. S. Chen, "Scattering from very rough metallic and dielectric surfaces: a theory based on the modified Kirchhoff approximation," *Waves in Random Media*, vol. 1, no. 1, pp. 21–34, 1991.

[5] S. L. Durden and J. F. Vesecky, "A numerical study of the separation wavenumber in the two-scale scattering approximation (ocean surface radar backscatter)," *IEEE Transactions on Geoscience and Remote Sensing*, vol. 28, no. 2, pp. 271-272, 1990.

[6] G. Soriano and C.-A. Guerin, "A cutoff invariant two-scale model in electromagnetic scattering from sea surfaces," *IEEE*

Geoscience and Remote Sensing Letters, vol. 5, no. 2, pp. 199–203, 2008.

[7] A. G. Voronovich, "Small-slope approximation in wave scattering from rough surfaces," *Journal of Experimental and Theoretical Physics*, vol. 62, no. 1, pp. 65–70, 1985.

[8] A. Voronovich, "Small-slope approximation for electromagnetic wave scattering at a rough interface of two dielectric half-spaces," *Waves in Random Media*, vol. 4, no. 3, pp. 337–367, 1994.

[9] G. Berginc, "Small-slope approximation method: a further study of vector wave scattering from two-dimensional surfaces and comparison with experimental data," *Progress in Electromagnetics Research*, vol. 37, pp. 251–287, 2002.

[10] A. Arnold-Bos, A. Khenchaf, and A. Martin, "Bistatic radar imaging of the marine environment-part I: theoretical background," *IEEE Transactions on Geoscience and Remote Sensing*, vol. 45, no. 11, pp. 3372–3383, 2007.

[11] Y. Zhao, X.-F. Yuan, M. Zhang, and H. Chen, "Radar scattering from the composite ship-ocean scene: facet-based asymptotical model and specular reflection weighted model," *IEEE Transactions on Antennas and Propagation*, vol. 62, no. 9, pp. 4810–4815, 2014.

[12] R. J. A. Tough and K. D. Ward, "The correlation properties of gamma and other non-Gaussian processes generated by memoryless nonlinear transformation," *Journal of Physics D: Applied Physics*, vol. 32, no. 23, pp. 3075–3084, 1999.

[13] H. T. Yura and S. G. Hanson, "Digital simulation of two-dimensional random fields with arbitrary power spectra and non-Gaussian probability distribution functions," *Applied Optics*, vol. 51, no. 10, pp. C77–C83, 2012.

[14] M. Rangaswamy, D. D. Weiner, and A. Ozturk, "Non-Gaussian random vector identification using spherically invariant random processes," *IEEE Transactions on Aerospace and Electronic Systems*, vol. 29, no. 1, pp. 111–124, 1993.

[15] T. J. Barnard and D. D. Weiner, "Non-Gaussian clutter modeling with generalized spherically invariant random vectors," *IEEE Transactions on Signal Processing*, vol. 44, no. 10, pp. 2384–2390, 1996.

[16] K. D. Ward, R. J. A. Tough, and S. Watts, *Sea Clutter: Scattering, the K Distribution and Radar Performance*, IET, Stevenage, UK, 2006.

[17] S. Watts, "Modeling and simulation of coherent sea clutter," *IEEE Transactions on Aerospace and Electronic Systems*, vol. 48, no. 4, pp. 3303–3317, 2012.

[18] G. Davidson, "Simulation of coherent sea clutter," *IET Radar, Sonar & Navigation*, vol. 4, no. 2, pp. 168–177, 2010.

[19] Y. Zhao, M. Zhang, H. Chen, and X.-F. Yuan, "Radar scattering from the composite ship-ocean scene: Doppler spectrum analysis based on the motion of six degrees of freedom," *IEEE Transactions on Antennas and Propagation*, vol. 62, no. 8, pp. 4341–4347, 2014.

[20] M. Zhang, Y. Zhao, J.-X. Li, and P.-B. Wei, "Reliable approach for composite scattering calculation from ship over a sea surface based on FBAM and GO-PO models," *IEEE Transactions on Antennas and Propagation*, vol. 65, no. 2, pp. 775–784, 2017.

[21] F. Yamazaki and M. Shinozuka, "Digital generation of non-Gaussian stochastic fields," *Journal of Engineering Mechanics*, vol. 114, no. 7, pp. 1183–1197, 1988.

[22] P. Zhou, X. Z. Zhang, P. K. Huang et al., "Results of airborne measurement of sea surface backscattering and analysis," *Systems Engineering and Electronics*, vol. 28, no. 3, pp. 325–328, 2006, in Chinese.

[23] G. Wu, Y. Liang, and S. Xu, "Numerical computational modeling of random rough sea surface based on JONSWAP spectrum and Donelan directional function," *Concurrency and Computation: Practice and Experience*, vol. e5514, 2019.

[24] T. Elfouhaily, B. Chapron, K. Katsaros, and D. Vandemark, "A unified directional spectrum for long and short wind-driven waves," *Journal of Geophysical Research: Oceans*, vol. 102, no. C7, pp. 15781–15796, 1997.

[25] L. Klein and C. Swift, "An improved model for the dielectric constant of sea water at microwave frequencies," *IEEE Transactions on Antennas and Propagation*, vol. 25, no. 1, pp. 104–111, 1977.